

Heterogeneous Nucleation and Growth of Nanoparticles at Environmental Interfaces

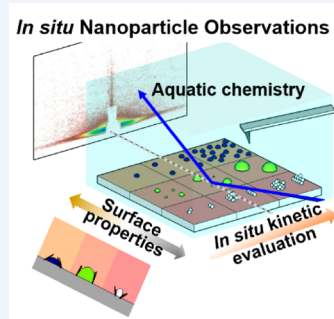
Young-Shin Jun,* Doyoon Kim, and Chelsea W. Neil[†]

Department of Energy, Environmental and Chemical Engineering, Washington University, St. Louis, Missouri 63130, United States

CONSPECTUS: Mineral nucleation is a phase transformation of aqueous components to solids with an accompanying creation of new surfaces. In this evolutional, yet elusive, process, nuclei often form at environmental interfaces, which provide remarkably reactive sites for heterogeneous nucleation and growth. Naturally occurring nucleation processes significantly contribute to the biogeochemical cycles of important components in the Earth's crust, such as iron and manganese oxide minerals and calcium carbonate. However, in recent decades, these cycles have been significantly altered by anthropogenic activities, which affect the aqueous chemistry and equilibrium of both surface and subsurface systems. These alterations can trigger the dissolution of existing minerals and formation of new nanoparticles (i.e., nucleation and growth) and consequently change the porosity and permeability of geomedia in subsurface environments.

Newly formed nanoparticles can also actively interact with components in natural and engineered aquatic systems, including those posing a significant hazard such as arsenic. These interactions can bilaterally influence the fate and transport of both newly formed nanoparticles and aqueous components. Due to their importance in natural and engineered processes, heterogeneous nucleation at environmental interfaces has started to receive more attention. However, a lack of time-resolved *in situ* analyses makes the evaluation of heterogeneous nucleation challenging because the physicochemical properties of both the nuclei and surfaces significantly and dynamically change with time and aqueous chemistry.

This Account reviews our *in situ* kinetic studies of the heterogeneous nucleation and growth behaviors of iron(III) (hydr)oxide, calcium carbonate, and manganese (hydr)oxide minerals in aqueous systems. In particular, we utilized simultaneous small-angle and grazing incidence small-angle X-ray scattering (SAXS/GISAXS) to investigate *in situ* and in real-time the effects of water chemistry and substrate identity on heterogeneously and homogeneously formed nanoscale precipitate size dimensions and total particle volume. Using this technique, we also provided a new platform for quantitatively comparing between heterogeneous and homogeneous nucleation and growth of nanoparticles and obtaining undiscovered interfacial energies between nuclei and surfaces. In addition, nanoscale surface characterization tools, such as *in situ* atomic force microscopy (AFM), were utilized to support and complement our findings. With these powerful nanoscale tools, we systematically evaluated the influences of environmentally abundant (oxy)anions and cations and the properties of environmental surfaces, such as surface charge and hydrophobicity. The findings, significantly enhanced by *in situ* observations, can lead to a more accurate prediction of the behaviors of nanoparticles in the environment and enable better control of the physicochemical properties of nanoparticles in engineered systems, such as catalytic reactions and energy storage.



1. IMPORTANCE OF HETEROGENEOUS NUCLEATION

Nanoparticle formation at environmental interfaces (heterogeneous nucleation) critically influences the fate and transport of aqueous species.¹ The specific surface area of particles, especially at nanoscale, increases drastically with decreasing particle size. The excess surface energy of nanoparticles, induced by the large surface volume fraction of atoms, drives high surface sorption to minimize the free energy state.² For example, during the early stages of iron(III) (hydr)oxide nanoparticle formation on mineral surfaces, toxic metals and oxyanions can be incorporated within the structure or adsorbed onto the surface of newly formed nanoparticles and finally immobilized.^{3,4} These phenomena more actively occur where aqueous chemistry changes abruptly, such as in acid-mine-drainage (AMD), nuclear accident sites, and energy-related exploration sites. Nanoparticles in aqueous environments, which either form naturally in solution (homogeneous nucleation) or are released from

engineered systems, can also act as heterogeneous nucleation sites, incorporating toxic or trace elements and molecules into a "hybrid" engineered/natural nanoparticle composite. These hybrid nanoparticles can travel long distances while their colloidal stability is maintained, making it difficult to predict their environmental impacts. The increasing emergence of natural, engineered, and hybrid nanoparticles makes it imperative to study their birth (i.e., nucleation) and impacts on the environment.⁵

The application of engineered solutions to mitigate environmental problems also affects heterogeneous nucleation. For example, during geologic carbon sequestration (GCS), CO₂ injection into deep saline aquifers can significantly decrease pH and increase carbonate concentrations.⁶ Alterations in aqueous chemistry can dissolve native minerals and form secondary

Received: May 1, 2016

Published: August 11, 2016

nanophases, possibly changing the pore structure of the subsurface system. This alteration of the pore-structure can govern the efficiency of GCS and potentially increase the risk of caprock cracking and gas leakage. Similarly, during managed aquifer recharge (MAR), one technical solution readily available to use reclaimed water to address water needs in areas where supplies are low, the injection of reclaimed water may trigger the dissolution of aquifer minerals, such as As-containing pyrite, and new nanoparticle formation.⁷ In this system, the modes (hetero- vs homogeneous) and extent of nucleation are important factors influencing the potential release and transport of toxic or heavy metal ions into recharged water, deteriorating the water quality.⁸

Furthermore, principles governing heterogeneous nucleation can be directly applied to the development of engineered nanomaterials, allowing us to utilize “green chemistry” approaches to synthesize nanoparticles with specific, controlled properties and reduce waste streams during manufacturing processes.⁹ Predicting the environmental impacts of nanoparticles, which are released from industry or form naturally in subsurface areas influenced by human activities, has become increasingly important. Thus, a better understanding of nanoparticle nucleation and growth will empower us to significantly advance our investigations into the life cycle of natural, engineered, and hybrid nanoparticles, protecting natural resources such as clean drinking water and mitigating global climate change.

2. TIME-RESOLVED *IN SITU* ANALYSIS OF THE NUCLEATION AND GROWTH KINETICS OF NANOPARTICLES

Because newly formed particles at mineral–water interfaces are often amorphous and hydrated, the evaluation of nucleation kinetics requires time-resolved *in situ* techniques. Previous nanoscale observations relied on snapshot images of these nanoparticles taken after sample preparation, which can significantly alter their physicochemical properties. Recent advances in *in situ* microscopic analysis can alleviate some challenges;^{10–12} however, these studies are still limited to accurately simulating aqueous environments in a narrow slit observation chamber or under cryogenic conditions. These limitations, therefore, prevent us from fully exploring the *in situ* kinetics and, in particular, heterogeneous nucleation on substrates during its initial stage.

This Account presents the progress our research group has made toward understanding the nucleation and growth of nanoparticles on mineral substrates in aqueous environments. The *in situ* experimental setup was developed by Jun et al.¹ to investigate water chemistry and substrate effects on nanoparticle precipitation in real-time, utilizing simultaneous small-angle and grazing incidence small-angle X-ray scattering (SAXS/GISAXS). For the analysis, a clean and flat substrate, such as well-polished quartz, is placed in the bottom of the reaction cell and aligned with the X-ray beam. Over the period of the reaction, images are

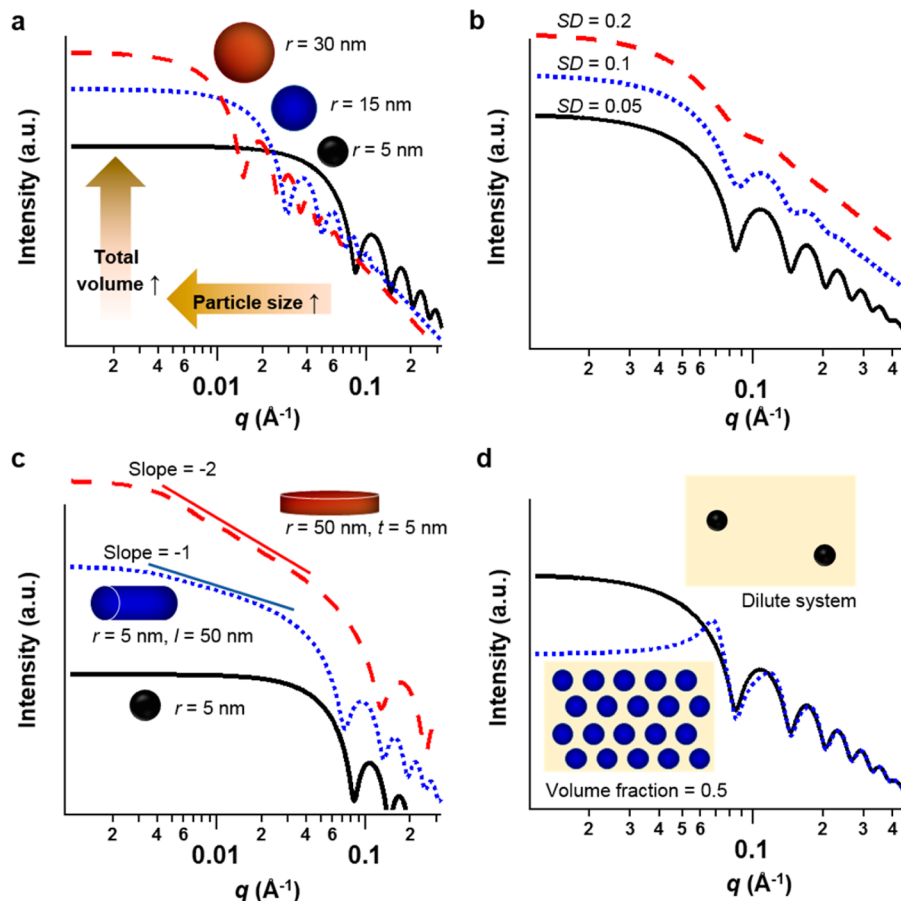


Figure 1. Schematic illustration showing how 1D SAXS patterns are changed by (a) particle size, (b) size distribution, and (c) particle morphology, and (d) particle volume fraction. Patterns were modeled using the Irena package.¹³ (a) Spheres with mean radius, r . (b) Spheres ($r = 5 \text{ nm}$) in log-normal distribution with standard deviation, SD . (c) Spheres ($r = 5 \text{ nm}$), cylinders ($r = 5 \text{ nm}$; length, $l = 50 \text{ nm}$), and discs ($r = 50 \text{ nm}$, thickness, $t = 5 \text{ nm}$). (d) Spheres ($r = 5 \text{ nm}$) in a dilute system (no structural factor influence) and a highly concentrated system with a volume fraction of 0.5.

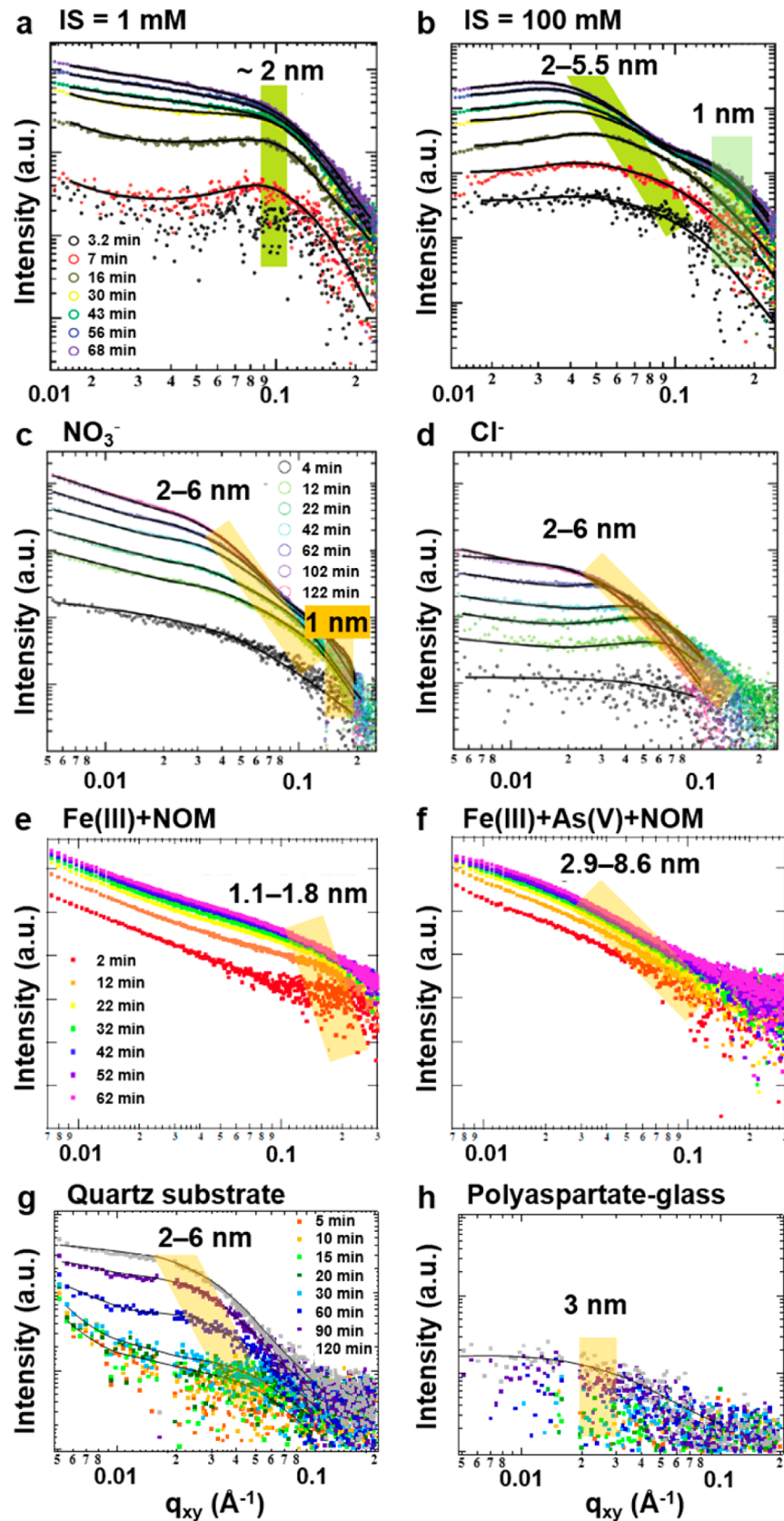


Figure 2. *In situ* measurements of heterogeneous nucleation on quartz substrates in solutions containing 10^{-4} M $\text{Fe}(\text{NO}_3)_3$ at $\text{pH } 3.6 \pm 0.2$ by GISAXS, showing in-plane (q_{xy}) 1D scattering. (a) With 1 mM NaNO_3 IS, nucleation is dominant. (b) With 100 mM NaNO_3 IS, particles grew from $\sim 2\text{--}5.5$ nm, with the formation of secondary ~ 1 nm particles. (c) With 10 mM NaNO_3 , both nucleation and growth were observed. (d) With 10 mM NaCl , although the particle size is comparable to the nitrate system, the total particle volume does not increase, indicating Ostwald ripening. (e) In the presence of NOM, particles aggregate, as indicated by power law scattering at low q . (f) In the presence of both arsenate and NOM, large particles are also observed.

taken of the solution (SAXS) and substrate (GISAXS) to observe the homogeneously and heterogeneously formed precipitates, respectively. For heterogeneous precipitation, the X-ray beam is passed over the substrate surface at a low incidence angle (α_i), which needs to be slightly smaller than critical angle (α_c) to enable highly surface sensitive detection.

As the beam is scattered by nanoparticles on the surface or in solution, characteristic 2D scattering images are collected by a detector and analyzed to yield information about the size, total volume, and number of particles. To confirm the absence of any discernible X-ray beam interactions, *in situ* samples, which experienced multiple scans at different sampling spots, were compared with pseudo-*in situ* samples, which were scanned only once. For further analysis, 2D patterns are reduced to 1D by cross-sectioning for both the horizontal and vertical dimensions. Cutting along the scattering pattern for each time point gives a series of curves plotting the intensity (I) versus the scattering vector (q , Å⁻¹). One-dimensional SAXS patterns changed by particle size, size distribution, form factor (morphology), and structural factor (particle–particle distance or volume fractions of particles) are illustrated in Figure 1.¹³ The q -position of the bend in this curve (e.g., highlighted positions of GISAXS patterns in Figure 2) is inversely related to the particle size (i.e., a larger q indicates a smaller particle size, as shown in Figure 1a). The invariant value ($Q = \int I(q)q^2 dq$) is linearly related to the total particle volume. The Guinier approximation, $I(q) = I(0) \times \exp(-q^2 R_g^2/3)$, can be used to fit the radius of gyration (R_g) of the randomly oriented nanoparticles. $I(0)$ is a quantity proportional to the total volume. The morphology and size distribution of particles can be determined by fitting 1D patterns using form and structure factors and size distribution functions. Approaches for the data collection and analysis can be slightly different based on the purpose of the study and characteristics of the nanoparticles. Thus, readers should seek detailed information in the original articles introduced in this Account. More information about X-ray scattering patterns based on nanoparticle behaviors can also be found in the literature.^{14,15}

By combining multiple surface characterization tools, such as atomic force microscopy (AFM), electron microscopies, contact angle analysis, and Raman spectroscopy, we investigated heterogeneous nucleation on geomedia, giving careful consideration to aqueous chemistry and surface properties. In particular, we have evaluated the behaviors of iron(III) (hydr)oxide, calcium carbonate, and manganese (hydr)oxide nanoparticles, which are abundant in the natural environment and important in engineering applications. Such *in situ* analysis, with the support of other techniques for phase identification and morphological information, can also be interpreted using classical nucleation theory (CNT) to provide important thermodynamic and kinetic insights into the early stage of nanoparticle formation.¹⁶ These studies contribute to our understanding of how aqueous environments determine the nucleation, growth, and aggregation of newly formed nanoparticles.

3. IRON(III) (HYDR)OXIDES

3.1. The Influence of Water Chemistry

Iron(III) (hydr)oxide nanoparticles are commonly produced by the weathering of iron-containing minerals or by anthropogenic activities at AMD or MAR sites.^{1,7,17} The propensity of these nanoparticles to act as natural sinks for aqueous contaminants will depend on characteristics such as their particle size, phase, and surface charge, as well as their formation location.

To quantitatively analyze *in situ* nucleation and growth, Jun et al.¹ developed an environmental SAXS/GISAXS setup to provide information on the effect of ionic strength (IS) on iron(III) (hydr)oxide nucleation and growth from solutions containing 10⁻⁴ M Fe(NO₃)₃ at pH 3.6. Comparable conditions can be found in AMD sites,¹⁷ GCS aquifers,⁶ and advanced oxidation processes (AOPs).¹⁸ Under these conditions, the volume of heterogeneous iron(III) (hydr)oxide nanoparticles on quartz dominated over homogeneous nanoparticles by a factor of 192. For the 1 mM IS system, there was active nucleation of particles with a ~2 nm radius but little growth (Figure 2a), which resulted from the stronger repulsion between iron(III) (hydr)-oxide monomers and quartz than that in systems with a higher IS. At IS = 100 mM, particles grew to 5.5 nm, and secondary ~1 nm particles formed within 1 h (Figure 2b). The secondary particles were hypothesized to be partially hydrolyzed ferric clusters that were attached to existing precipitates.

In addition to the IS, anions also strongly influence the nucleation and growth of iron(III) (hydr)oxide. Hu et al. reported the effect of three different salts (NaNO₃, NaCl, and Na₂SO₄).¹⁹ Under the same pH, IS, and saturation conditions, the total particle volume formed on quartz decreased by 10 times in the chloride system compared with the nitrate system, because of ferric ion complexation by chloride (Figure 2c,d).^{19,20} The constant total particle volume with growing size in the chloride system indicated that particles grew through Ostwald ripening, while particles in the nitrate systems underwent continuous nucleation and growth. For the sulfate system, there was very fast growth and aggregation due to the neutralized surface charge of the iron(III) (hydr)oxide. Neil et al.²¹ examined the effects of arsenate and phosphate (the dominant species are H₂AsO₄⁻ and H₂PO₄⁻ at pH 3.6) and found that arsenate and phosphate oxyanion incorporation into iron(III) (hydr)oxide nuclei decreased their crystallinity and increased their water content. As a result, the total particle volumes in oxyanion-containing systems were larger but particles were fewer in number than in the system without oxyanions. The influence of anions on the nucleation and growth of nanoparticles can also be significantly altered by natural organic matter (NOM). Our most recent study evaluated the nucleation and aggregation behavior of iron(III) (hydr)oxides in a ternary system of Fe(III)–arsenate–NOM.²² In this system, Fe(III) initially interacts with NOM in solution to form fractal aggregates (linear power law scattering at low q , Figure 2e). Arsenate can then disaggregate the fractal aggregates, resulting in particle growth similar to systems where NOM is absent (Figure 2f). The impacts of cations were also studied. For example, Hu et al.²³ observed that Al(III) slowed iron (hydr)oxide nanoparticle growth by changing the surface charge of quartz substrates from negative to positive, increasing the electrostatic repulsive forces, which repelled iron(III) (hydr)-oxide monomers. Al(III) also delayed Ostwald ripening of the nanoparticles.

3.2. The Influence of Surface Properties of Substrates

The effects of the substrate on iron(III) (hydr)oxide formation were tested by Hu et al.²⁴ For this study, the quartz (α -SiO₂) surface was compared with two other earth-abundant minerals with distinct surface properties, muscovite (mica, KAl₂(Si₃Al)-O₁₀(OH,F)₂) and corundum (α -Al₂O₃). We observed that corundum had both the fastest nucleation and slowest growth of iron(III) (hydr)oxide. Electrostatic forces between the substrate and positively charged iron(III) (hydr)oxide polymeric embryos resulted in faster growth for negatively charged

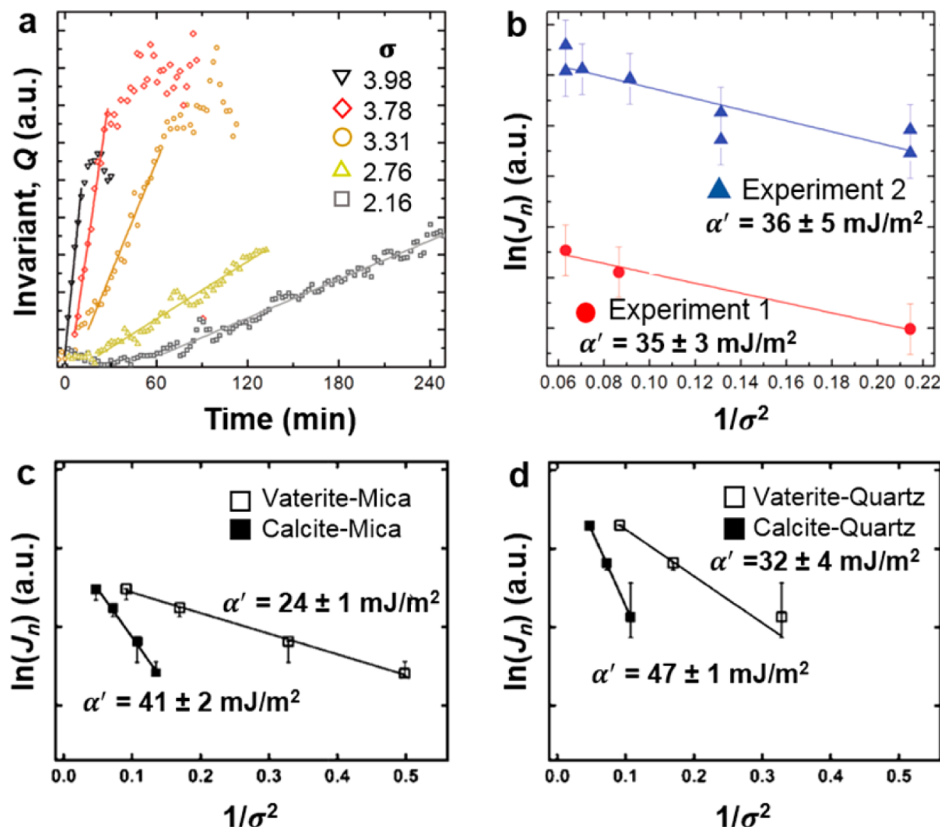


Figure 3. (a) Evolution of the invariant with time at different calcite supersaturations (σ) for the evaluation of heterogeneous CaCO_3 nucleation on quartz. (b) The obtained nucleation rates and the $1/\sigma^2$ show a good linear relationship, thus the effective interfacial energy can be fitted. The data from two different synchrotron runs are shown. (c,d) Effective interfacial energies of CaCO_3 –mica and CaCO_3 –quartz systems. Reproduced from refs 29 and 30. Copyrights 2013 and 2014 American Chemical Society.

substrates (mica and quartz). On the other hand, nucleation was controlled by interfacial energies. Corundum had the highest substrate–water interfacial energy, as indicated by the highest water contact angle. Corundum also had the lowest precipitate–substrate interfacial energy, because it had least metal–oxygen and oxygen–oxygen bond length mismatch with iron(III) (hydr)oxides. Thus, corundum posed the lowest energy barrier to heterogeneous nucleation, and the system consequently had the fastest nucleation.

To investigate the effect of organic surface coatings, which are abundant in natural and engineered systems, Ray et al.²⁵ compared the heterogeneous precipitation of iron(III) (hydr)oxides on quartz to that on polyaspartate- and alginate-coated glass. Despite the more negative surface charge in polyaspartate-coated systems, less precipitation was observed than on quartz (Figures 2g,h). Thus, on organic-coated substrates, rather than electrostatics, the degree of surface hydrophilicity controlled the nucleation and growth, because increased hydrophobicity of organic-coated substrates can increase the interfacial energy between the nanoparticles and substrate. Nucleation and growth occurred more quickly on the most hydrophilic surface, quartz, than on the least hydrophilic surface, polyaspartate.

3.3. Implications for Iron(III) (Hydr)oxide Nanoparticles in Engineered Systems

Through our studies on iron(III) (hydr)oxide nanoparticle formation, we have discovered several mechanisms at the heart of nucleation and growth behavior, which can be applied to other systems. For example, iron(III) (hydr)oxides can impact the stability of engineered CeO_2 nanoparticles released into natural

and engineered aqueous systems through the formation of hybrid nanoparticles. Liu et al.²⁶ investigated the fate and transport of CeO_2 nanoparticles in the presence of Fe(II). Redox reactions between CeO_2 and Fe(II) under anaerobic conditions formed six-line ferrihydrite on the CeO_2 surface, which increased the ζ potential and surface hydrophilicity.²⁷ Consequently, the colloidal stability of CeO_2 was significantly enhanced.

4. CALCIUM CARBONATES (CaCO_3)

4.1. In Situ Studies of the Kinetic and Thermodynamic Aspects of CaCO_3 Nucleation

Calcium carbonate minerals are important in subsurface environments due to their abundance and impacts on aqueous chemistries and geomechanical and hydrogeological properties.²⁸ An increasing number of recent studies have reported nonclassical pathways of nucleation and growth for CaCO_3 ,^{11,16} demanding more accurate evaluations. Utilizing SAXS/GISAXS, our group has explored nanoscale CaCO_3 formation kinetics at environmental interfaces. The first *in situ* CaCO_3 study utilizing GISAXS was conducted by Fernandez-Martinez et al.²⁹ to provide quantitative parameters, such as nucleus size and interfacial energies, for reactive transport models with nucleation as an explicit step. This study determined the interfacial energies controlling the heterogeneous nucleation of CaCO_3 on quartz (100) surfaces. According to CNT, the nucleation rate, J_n , can be expressed by an exponential term including a supersaturation term ($\sigma = \ln(\text{IAP}/K_{\text{sp}})$, where IAP is the ion activity product and K_{sp} is the solubility product) as the driving

force to overcome the nucleation energy barrier (Δg_n), as shown in eq 1.

$$\begin{aligned} J_n &= A \exp(-\Delta g_n/(k_B T)) \\ &= A \exp(-16\pi v_m^2 \alpha'^3 / (3k_B^3 T^3 \sigma^2)) \end{aligned} \quad (1)$$

$$\ln(J_n) = J_0 - B/\sigma^2 \quad (2)$$

$$B = 16\pi v_m^2 \alpha'^3 / (3k_B^3 T^3) \quad (3)$$

Here, A is a kinetic factor related to activation energy. Because all but one of the components in B are known values (v_m is the molecular volume, k_B is the Boltzmann constant, and T is the absolute temperature), the effective interfacial energy, α' , can be calculated from the linear fitting of the relationship between the natural log of the nucleation rate, $\ln(J_n)$, and $1/\sigma^2$. By measuring nucleation rates at different σ , (Figure 3a), the α' can be obtained (Figure 3b).

From *in situ* GISAXS experiments, we obtained the nucleation rates of CaCO_3 on substrates, J_n , directly from Q (when growth is negligible, showing a uniform particle size) or by a fitting method with consideration of particle size evolution.³⁰ Using this approach, we obtained a value of $\alpha' = 36 \pm 5 \text{ mJ/m}^2$ for the effective interfacial free energy governing the heterogeneous nucleation of CaCO_3 (assuming calcite), which is significantly lower than the interfacial energy governing homogeneous nucleation ($\alpha \approx 120 \text{ mJ/m}^2$), suggesting that heterogeneous CaCO_3 nucleation is favored on quartz under the

experimental conditions. Li et al.³⁰ further developed this study by obtaining interfacial energies for heterogeneous nucleation on both mica and quartz with respect to both calcite and vaterite polymorphs. The α' was $24 \pm 1 \text{ mJ/m}^2$ for the vaterite–mica interface and $32 \pm 4 \text{ mJ/m}^2$ for the vaterite–quartz interface (Figures 3c,d). The smaller α' of the CaCO_3 –mica interface led to smaller particles and often higher particle densities on mica. After considering three substrate-related factors, structure (bond length) mismatch between the substrate and the precipitate, the extent of hydrophilicity, and the surface charge of the substrate surfaces, Li et al. suggested that the better structural compatibility between CaCO_3 and mica than between CaCO_3 and quartz contributed to the decreased α' in the system.³⁰ Thus, the interfacial energy relationship plays a more significant role in CaCO_3 nucleation and growth than the surface charge does. The findings of this study provide new thermodynamic parameters for subsurface reactive transport modeling and contribute to our understanding of CaCO_3 formation mechanisms on environmental surfaces.

4.2. Implications of CaCO_3 Nucleation for GCS Sites

One engineered system where CaCO_3 formation is a concern is wellbore cement installed for GCS. During GCS operation, CO_2 is injected into a geologic formation through injection wells, whose liners are cast using concrete containing Portland cement. Hardened cement, which mainly consists of calcium silicate hydrates and portlandite ($\text{Ca}(\text{OH})_2$), has a pH above 12.5. Injection of CO_2 produces carbonic acid in the presence of water,

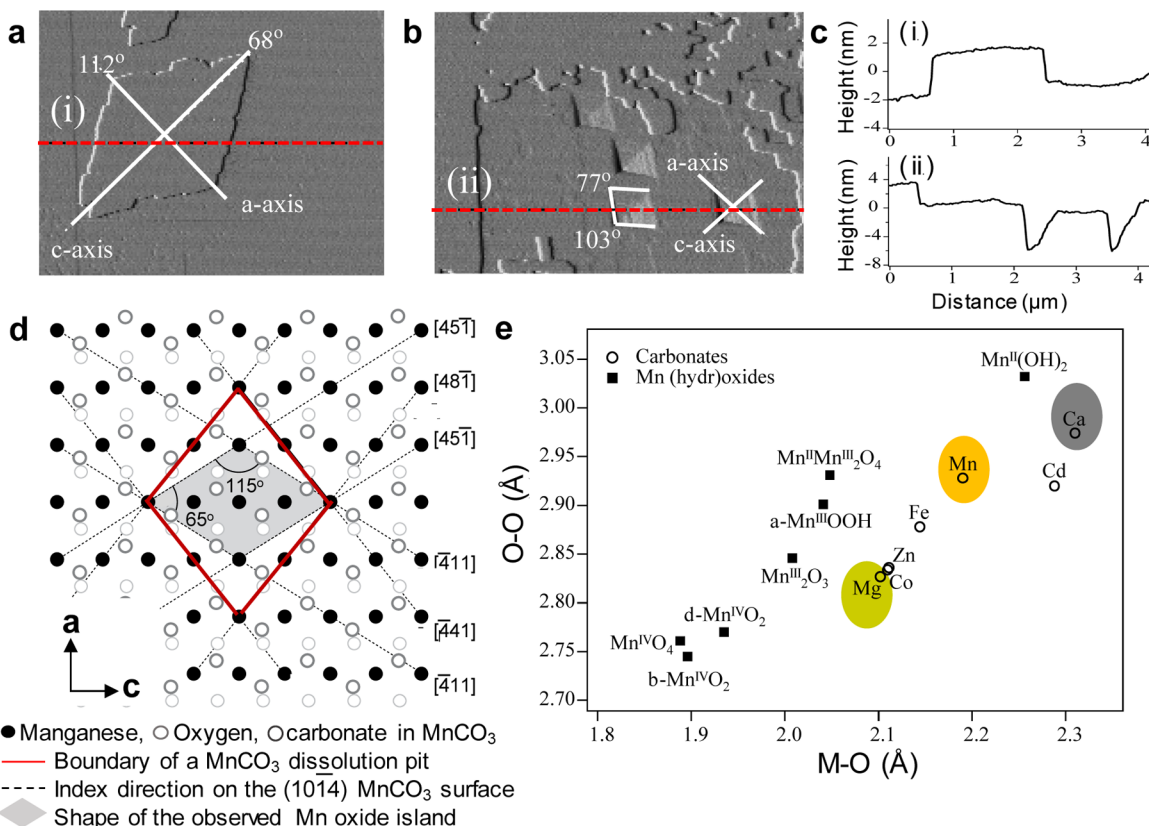


Figure 4. (a,b) *In situ* AFM micrographs ($4.7 \times 3.3 \mu\text{m}^2$) of simultaneous substrate dissolution of MnCO_3 and manganese oxide island formation at pH 6.1. (a) A rhombus-shaped island after 120 min in solution. The island grew with a 90° rotation relative to the crystallographic axis of the substrate. (b) Coalescence of islands, forming a film, after 950 min, and contemporaneous appearance of many dissolution pits. (c) Height profiles along the dotted lines in AFM images from panels a and b. (d) Hypothesized positioning of the manganese oxide island on a manganese carbonate substrate. (e) Comparison of the oxygen–oxygen and metal–oxygen bond lengths of rhombohedral carbonates. Reproduced from ref 33. Copyright 2005 American Chemical Society.

leading to $\text{CO}_2(\text{aq})$ attack on the well cement, which affects the efficiency and safety of GCS. To provide information on wellbore cement integrity, Li et al.³¹ analyzed chemical and mechanical alterations of cement samples reacted for 10 days under GCS conditions (95 °C and 100 bar, IS = 0.5 M). Chemical analyses showed that the cement samples were significantly attacked by $\text{CO}_2(\text{aq})$, forming CaCO_3 in their microcracks ($\text{Ca}(\text{OH})_2(\text{s}) + \text{CO}_2(\text{aq}) \rightarrow \text{CaCO}_3(\text{s}) + \text{H}_2\text{O}$). With a total attacked depth of 1220 μm , the strength and elastic modulus of the bulk cement samples were reduced by 93% and 84%, respectively. The formation of CaCO_3 can exert a complex influence on the layer structure, microcracks, and swelling of the outer layers, and affect CO_2 intrusion. On the contrary, if this carbonated layer is weak and defective, CO_2 attack cannot be effectively hindered, and severe deterioration in the cement's mechanical properties is expected. Therefore, considering the crucial role of the carbonated layer, it is necessary to better understand carbonate formation in porous media, and its consequential influences on the physicochemical properties of the geomedia.

5. MANGANESE (HYDR)OXIDES

Manganese redox cycling and the accompanying dissolution and precipitation reactions are important processes in natural waters, especially at oxic/anoxic transition zones.³² In addition, bioavailable manganese is essential for all life forms as a principal cofactor in many enzymes. Therefore, the study of manganese (hydr)oxide heterogeneous nucleation at environmental interfaces can improve predictive models of the fate and transport of nutrients and contaminants. Jun et al.³³ observed heteroepitaxial growth of manganese oxide islands on the (1014) surface of MnCO_3 through the $\text{Mn}^{2+}(\text{aq})$ reaction with $\text{O}_2(\text{aq})$ at pH 6.1 in oxygen saturated aqueous systems (Figure 4a). Heteroepitaxy refers to the layer growth of a different material on top of a substrate. The islands grew laterally to several square micrometers before separate islands collided and coalesced, but they did not grow over substrate steps or down dissolution pit edges (Figure 4b). Their heights were self-limited to 2–3 nm (Figure 4c). On terraces, rhombus-shaped manganese oxide islands formed under the influence of the crystallographic axis of the underlying carbonate substrate (Figure 4d). A line bisecting

the acute angles of the oxide island is coplanar with the *c*-glide plane of the rhodochrosite crystal structure of MnCO_3 . Those behaviors were explained by a free energy model, including stress and strain between manganese oxide nanofilms and MnCO_3 substrates. Similar heteroepitaxial growth of manganese oxide was observed on the surface of MgCO_3 , but not on the surface of CaCO_3 . This difference resulted from the relative bond length mismatch between the atomic structures of the carbonate substrates and manganese oxides (Figure 4e).

In engineering processes, such as manganese remediation sites, manganese (hydr)oxide formation is favorable at high pH. Jung and Jun³⁴ investigated the heterogeneous nucleation and growth of manganese (hydr)oxide on the (100) surface of quartz as a representative environmental interface. The (100) surface of quartz is commonly exposed in nature. The experimental conditions (pH 10.1, 0.1 mM Mn^{2+} , 1–100 mM IS) were chosen to simulate acid mine drainage remediation sites, where high pH conditions are frequently reported during Mn mitigation. They found that IS controls $\text{Mn}(\text{OH})_2(\text{aq})$ formation by affecting the system's saturation and subsequently the formation of round $\text{Mn}(\text{OH})_2(\text{s})$ and rod-shaped $\text{Mn}_3\text{O}_4(\text{s})$ nanoparticles. In the 100 mM IS system, heterogeneously nucleated manganese (hydr)oxide particles covered more of the quartz substrate than those in the 1 and 10 mM IS systems. In sum, this high IS decreased the activity of Mn^{2+} ions, lowering the supersaturation ratio of $\text{Mn}(\text{OH})_2(\text{s})$ and promoting heterogeneous manganese (hydr)oxide nucleation on quartz (eq 1). Based on more heterogeneous nucleation and their larger horizontal than vertical dimension at high IS, nuclei may have a better structural compatibility with the quartz substrate, resulting in later homoepitaxial manganese (hydr)oxide growth (i.e., growth on top of a substrate of the same material, Figure 5). Based on these findings, one can infer that, at higher IS, the heterogeneous nucleation of manganese (hydr)oxide increases the surface area of newly formed particles, where the reactivity can be higher than on bare substrates, such as quartz.

6. CONCLUSIONS AND OUTLOOK

Recent studies have made great achievements in characterizing the molecular structures of environmental interfaces to expand

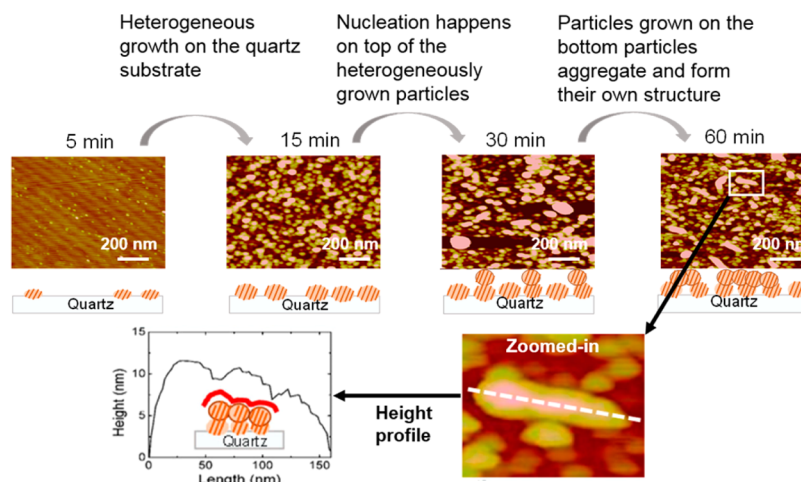


Figure 5. AFM height images ($1 \times 1 \mu\text{m}^2$) of manganese (hydr)oxide nucleated on a quartz (10^{-4} M Mn(II), 100 mM IS, and pH 10.1) at 5–60 min. The schematic drawings explain the heterogeneous nucleation of manganese (hydr)oxide on the quartz, followed by the nucleation and growth on top of the heterogeneously nucleated particles. The nucleated particles formed both rod-shaped and round particles through oriented aggregation. A zoomed-in image at 60 min and its height profiles along the white dotted line supports the existence of secondary nucleation. Reproduced from ref 34. Copyright 2016 American Chemical Society.

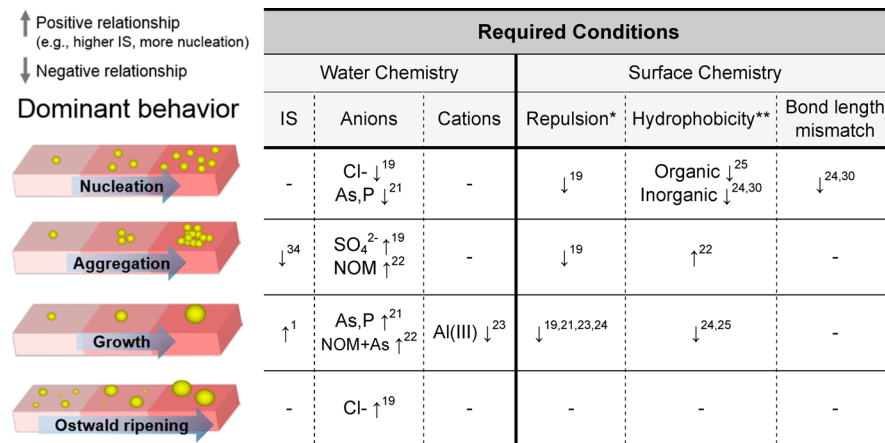


Figure 6. Factors influencing the nucleation and growth behaviors discussed in this Account. Numbers are cited references. *Repulsive force was evaluated by measuring the surface charge differences between the substrate and the nuclei. **Hydrophobicity was evaluated by analyzing the contact angle between the surface of the substrate and water. The influence of NOM was studied with anions in ref 22, thus indicated in the anions column.

our understanding about geochemical processes such as nutrient availability, biominerization, and soil formation and weathering.³⁵ For more than two decades, *in situ* techniques, such as AFM and transmission electron microscopy, have enabled direct observations at nanoscale.^{11,36}

In this Account, we reviewed the diverse heterogeneous nucleation and growth behaviors of nanoparticles at aqueous environmental interfaces, with special consideration given to kinetic and thermodynamic characteristics. The approaches introduced here are powerful because the samples are not dehydrated for observation. They provide a high spatiotemporal resolution with improved statistics by using a larger sample scanning size (centimeter scale rather than nano- or micrometer scale). Observations under fully hydrated conditions are important because water molecules around nanoparticle surfaces are often well-ordered compared with their bulk counterparts and the extent of nanoparticle hydration can affect their thermodynamics.³⁷ Using this approach, we have begun to provide new interfacial energy values between newly formed hydrated nuclei and substrates.

Minerals of interest were studied under different environmental testing conditions, such as pH and IS. For example, iron (hydr)oxides were studied mainly under acidic conditions, while calcium carbonate and manganese (hydr)oxide were evaluated under neutral to basic conditions. Furthermore, different aspects of nucleation were considered for each mineral; for example, we considered fractal aggregation of iron (hydr)oxide,²² polymorphs of calcium carbonate,³⁰ and redox chemistry-triggered formation of manganese (hydr)oxide.³² Despite these complexities, we found that the nucleation and growth behaviors of these minerals could be explained in general aqueous and interfacial chemistry terms, closely related to nucleation theories. For example, structural compatibility between nuclei and substrate minerals was an important factor for all three minerals.^{24,30,34} We also commonly observed more dominant growth when repulsive forces between substrates and nucleation monomers were weaker (Figure 6).^{19,21,23,24} However, when complex aqueous factors coexist, it is crucial to have a more holistic evaluation to determine which factors are most important for different nanoparticles.

In addition, more careful consideration of the morphology of nuclei will be required. Most studies, including our own, assume spherical or hemispherical particle morphology during the application of CNT. However, as manganese oxide formed

on manganese carbonate shows (Figure 4a), many environmental minerals have faceted morphologies, which SAXS/GISAXS analysis can successfully resolve. Faceted minerals have a higher possibility of undergoing phase transformation from amorphous to crystalline phases, and reactivities can be different at specific faceted surfaces.¹¹

By coupling our approach with recent advances in surface characterization techniques, the understanding of heterogeneous nucleation can be further improved. For example, GISAXS can be operated in conjunction with *in situ* grazing incidence wide angle scattering (GIWAXS), which can provide structural information about newly formed nanoparticles in aqueous systems. Similarly, *in situ* TEM can be used to provide real-time identification of polymorphs.¹¹ Atom probe tomography, an emerging technology, can be used to analyze the chemical compositions of geologic samples.³⁸ Combining these new techniques with the approaches described in this Account will be synergistic to further reveal the mechanisms behind heterogeneous nucleation.

As discussed above, an improved understanding of heterogeneous nucleation will allow us to better predict the fate and transport of nanoparticles in the environment and provide important parameters for reactive transport modeling of engineered subsurface systems. Nutrient management will benefit from a better estimate of the nucleation and dissolution of phosphorus minerals influenced by organic matter in fertilized soils or eutrophic aqueous environments. Moreover, the principles derived from our studies can be more broadly applied. For example, heterogeneous nucleation on surfaces has a number of industrial applications, such as catalytic reactions for energy conversion. Utilizing insights from nucleation studies, this process can be optimized to minimize the inputs of resources and time. In addition, natural resources, such as atmospheric oxygen, carbon dioxide, and sunlight, can be effectively used to form desired products, harnessing more environmentally benign reaction pathways and minimizing detrimental environmental impacts.

AUTHOR INFORMATION

Corresponding Author

*Mailing address: One Brookings Drive, Campus Box 1180, Washington University, St. Louis, Missouri 63130, United States. E-mail: ysjun@seas.wustl.edu. Phone: (314)935-4539. Fax: (314)935-7211. Web site: <http://encl.engineering.wustl.edu/>.

Present Address

[†]C.W.N.: Office of Research and Development, National Risk Management Research Laboratory, U.S. Environmental Protection Agency, Cincinnati, Ohio 45268, United States.

Notes

The authors declare no competing financial interest.

Biographies

Dr. Young-Shin Jun is the Harold D. Jolley Career Development Associate Professor of the Department of Energy, Environmental & Chemical Engineering (EECE) at Washington University in Saint Louis (WUSTL), where she leads the Environmental NanoChemistry Laboratory. Prior to her position at WUSTL, she conducted postdoctoral research at the University of California at Berkeley and Lawrence Berkeley National Laboratory (2005–2007). She holds a Ph.D. in Environmental Chemistry from Harvard University (2005).

Mr. Doyoon Kim received his B.S. degree in Civil Engineering (2009) and an M.S. degree in Environmental Engineering (2011) from Hanyang University, South Korea. He is pursuing his Ph.D. degree under the supervision of Prof. Young-Shin Jun at WUSTL. His research interests include nucleation behaviors of biomaterials in multiscale porous media.

Dr. Chelsea W. Neil received her B.S. degree in Chemical Engineering from Tufts University in 2010 and her Ph.D. in EECE from WUSTL in 2015, where she worked under the supervision of Prof. Young-Shin Jun to study arsenopyrite geochemical reactions during groundwater recharge. She is currently a postdoctoral researcher in the Water Supply and Water Resources Division of the US Environmental Protection Agency's Office of Research and Development.

ACKNOWLEDGMENTS

We are grateful for support received from National Science Foundation (Grants EAR-1424927 and CHE-1214090). This is also partially supported by the Center for Nanoscale Control of Geologic CO₂, an Energy Frontier Research Center funded by the U.S. Department of Energy, Office of Science, Office of Basic Energy Sciences under Award Number DE-AC02-05CH11231. We thank Environmental NanoChemistry Group members for valuable discussion and review. Use of the Advanced Photon Source (Sector 12 ID-B for SAXS/GISAXS) at Argonne National Laboratory was supported by the U.S. Department of Energy, Office of Science, Office of Basic Energy Sciences, under Contract No. DE-AC02-06CH11357.

REFERENCES

- (1) Jun, Y.-S.; Lee, B.; Waychunas, G. A. *In Situ* Observations of Nanoparticle Early Development Kinetics at Mineral–Water Interfaces. *Environ. Sci. Technol.* **2010**, *44*, 8182–8189.
- (2) Banfield, J. F.; Zhang, H. Nanoparticles in the environment. *Rev. Mineral. Geochem.* **2001**, *44*, 1–58.
- (3) Hochella, M. F.; Lower, S. K.; Maurice, P. A.; Penn, R. L.; Sahai, N.; Sparks, D. L.; Twinning, B. S. Nanominerals, Mineral Nanoparticles, and Earth Systems. *Science* **2008**, *319*, 1631–1635.
- (4) Lowry, G. V.; Hotze, E. M.; Bernhardt, E. S.; Dionysiou, D. D.; Pedersen, J. A.; Wiesner, M. R.; Xing, B. Environmental occurrences, behavior, fate, and ecological effects of nanomaterials: an introduction to the special series. *J. Environ. Qual.* **2010**, *39*, 1867–1874.
- (5) Lowry, G. V.; Gregory, K. B.; Apte, S. C.; Lead, J. R. Transformations of Nanomaterials in the Environment. *Environ. Sci. Technol.* **2012**, *46*, 6893–6899.
- (6) Jun, Y.-S.; Gianniaro, D. E.; Werth, C. J. Impacts of Geochemical Reactions on Geologic Carbon Sequestration. *Environ. Sci. Technol.* **2013**, *47*, 3–8.
- (7) Neil, C. W.; Yang, Y. J.; Jun, Y.-S. Arsenic Mobilization and Attenuation by Mineral-Water Interactions: Implications for Managed Aquifer Recharge. *J. Environ. Monit.* **2012**, *14*, 1772–1788.
- (8) Neil, C. W.; Yang, Y. J.; Schupp, D.; Jun, Y.-S. Water Chemistry Impacts on Arsenic Mobilization from Arsenopyrite Dissolution and Secondary Mineral Precipitation: Implications for Managed Aquifer Recharge. *Environ. Sci. Technol.* **2014**, *48*, 4395–4405.
- (9) Clark, J. H. Green Chemistry: Challenges and Opportunities. *Green Chem.* **1999**, *1*, 1–8.
- (10) Li, D.; Nielsen, M. H.; Lee, J. R. I.; Frandsen, C.; Banfield, J. F.; De Yoreo, J. J. Direction-Specific Interactions Control Crystal Growth by Oriented Attachment. *Science* **2012**, *336*, 1014–1018.
- (11) Nielsen, M. H.; Aloni, S.; De Yoreo, J. J. *In situ* TEM Imaging of CaCO₃ Nucleation Reveals Coexistence of Direct and Indirect Pathways. *Science* **2014**, *345*, 1158–1162.
- (12) Nudelman, F.; Pieterse, K.; George, A.; Bomans, P. H. H.; Friedrich, H.; Brylka, L. J.; Hilbers, P. A. J.; de With, G.; Sommerdijk, N. A. J. M. The Role of Collagen in Bone Apatite Formation in the Presence of Hydroxyapatite Nucleation Inhibitors. *Nat. Mater.* **2010**, *9*, 1004–1009.
- (13) Ilavsky, J.; Jemian, P. R. Irena: Tool Suite for Modeling and Analysis of Small-Angle Scattering. *J. Appl. Crystallogr.* **2009**, *42*, 347–353.
- (14) Beauchage, G.; Kammler, H. K.; Pratsinis, S. E. Particle Size Distributions from Small-Angle Scattering using Global Scattering Functions. *J. Appl. Crystallogr.* **2004**, *37*, 523–535.
- (15) Li, T.; Senesi, A. J.; Lee, B. Small Angle X-ray Scattering for Nanoparticle Research. *Chem. Rev.* **2016**, DOI: 10.1021/acs.chemrev.Sb00690.
- (16) De Yoreo, J. J.; Waychunas, G. A.; Jun, Y.-S.; Fernandez-Martinez, A. *In situ* Investigations of Carbonate Nucleation on Mineral and Organic Surfaces. *Rev. Mineral. Geochem.* **2013**, *77*, 229–257.
- (17) Ganguli, P. M.; Mason, R. P.; Abu-Saba, K. E.; Anderson, R. S.; Flegal, A. R. Mercury Speciation in Drainage from the New Idria Mercury Mine, California. *Environ. Sci. Technol.* **2000**, *34*, 4773–4779.
- (18) Andreozzi, R.; Caprio, V.; Insola, A.; Marotta, R. Advanced Oxidation Processes (AOP) for Water Purification and Recovery. *Catal. Today* **1999**, *53*, 51–59.
- (19) Hu, Y.; Lee, B.; Bell, C.; Jun, Y.-S. Environmentally Abundant Anions Influence the Nucleation, Growth, Ostwald Ripening, and Aggregation of Hydrous Fe(III) Oxides. *Langmuir* **2012**, *28*, 7737–7746.
- (20) Bottero, J. Y.; Tchoubar, D.; Arnaud, M.; Quienne, P. Partial Hydrolysis of Ferric Nitrate Salt. Structural investigation by Dynamic Light Scattering and Small-Angle X-ray Scattering. *Langmuir* **1991**, *7*, 1365–1369.
- (21) Neil, C. W.; Lee, B.; Jun, Y.-S. Different Arsenate and Phosphate Incorporation Effects on the Nucleation and Growth of Iron(III) (Hydr)oxides on Quartz. *Environ. Sci. Technol.* **2014**, *48*, 11883–11891.
- (22) Neil, C. W.; Ray, J. R.; Lee, B.; Jun, Y.-S. Fractal Aggregation and Disaggregation of Newly Formed Iron(III) (Hydr)oxide Nanoparticles in the Presence of Natural Organic Matter and Arsenic. *Environ. Sci.: Nano* **2016**, *3*, 647–656.
- (23) Hu, Y.; Li, Q.; Lee, B.; Jun, Y.-S. Aluminum Affects Heterogeneous Fe(III) (Hydr)oxide Nucleation, Growth, and Ostwald Ripening. *Environ. Sci. Technol.* **2014**, *48*, 299–306.
- (24) Hu, Y.; Neil, C.; Lee, B.; Jun, Y.-S. Control of Heterogeneous Fe(III) (Hydr)oxide Nucleation and Growth by Interfacial Energies and Local Saturation. *Environ. Sci. Technol.* **2013**, *47*, 9198–9206.
- (25) Ray, J. R.; Lee, B.; Baltrusaitis, J.; Jun, Y.-S. Formation of Iron(III) (Hydr)oxides on Polyaspartate- and Alginate-Coated Substrates: Effects of Coating Hydrophilicity and Functional Group. *Environ. Sci. Technol.* **2012**, *46*, 13167–13175.
- (26) Liu, X.; Ray, J. R.; Neil, C. W.; Li, Q.; Jun, Y.-S. Enhanced Colloidal Stability of CeO₂ Nanoparticles by Ferrous Ions: Adsorption, Redox Reaction, and Surface Precipitation. *Environ. Sci. Technol.* **2015**, *49*, 5476–5483.
- (27) Grassian, V. H.; Hamers, R. J. Nanomaterials and the Environment: The Chemistry and Materials Perspective., National

Science Foundation Workshop Report; Arlington, 2011; <https://nsfenv-nano.chem.wisc.edu/>.

- (28) Morse, J. W.; Arvidson, R. S.; Lüttge, A. Calcium Carbonate Formation and Dissolution. *Chem. Rev.* **2007**, *107*, 342–381.
- (29) Fernandez-Martinez, A.; Hu, Y.; Lee, B.; Jun, Y.-S.; Waychunas, G. A. In Situ Determination of Interfacial Energies between Heterogeneously Nucleated CaCO_3 and Quartz Substrates: Thermodynamics of CO_2 Mineral Trapping. *Environ. Sci. Technol.* **2013**, *47*, 102–109.
- (30) Li, Q.; Fernandez-Martinez, A.; Lee, B.; Waychunas, G. A.; Jun, Y.-S. Interfacial Energies for Heterogeneous Nucleation of Calcium Carbonate on Mica and Quartz. *Environ. Sci. Technol.* **2014**, *48*, 5745–5753.
- (31) Li, Q.; Lim, Y. M.; Flores, K. M.; Kranjc, K.; Jun, Y.-S. Chemical Reactions of Portland Cement with Aqueous CO_2 and Their Impacts on Cement's Mechanical Properties under Geologic CO_2 Sequestration Conditions. *Environ. Sci. Technol.* **2015**, *49*, 6335–6343.
- (32) Jun, Y.-S.; Martin, S. T. Microscopic Observations of Reductive Manganite Dissolution under Oxic Conditions. *Environ. Sci. Technol.* **2003**, *37*, 2363–2370.
- (33) Jun, Y.-S.; Kendall, T. A.; Martin, S. T.; Friend, C. M.; Vlassak, J. J. Heteroepitaxial Nucleation and Oriented Growth of Manganese Oxide Islands on Carbonate Minerals under Aqueous Conditions. *Environ. Sci. Technol.* **2005**, *39*, 1239–1249.
- (34) Jung, H.; Jun, Y.-S. Ionic Strength-Controlled Mn (Hydr)oxide Nanoparticle Nucleation on Quartz: Effect of Aqueous $\text{Mn}(\text{OH})_2$. *Environ. Sci. Technol.* **2016**, *50*, 105–113.
- (35) Putnis, C. V.; Ruiz-Agudo, E. The Mineral–Water Interface: Where Minerals React with the Environment. *Elements* **2013**, *9*, 177–182.
- (36) Dove, P. M.; Hochella, M. F. Calcite precipitation mechanisms and inhibition by orthophosphate: In situ observations by Scanning Force Microscopy. *Geochim. Cosmochim. Acta* **1993**, *57*, 705–714.
- (37) Navrotsky, A.; Mazeina, L.; Majzlan, J. Size-Driven Structural and Thermodynamic Complexity in Iron Oxides. *Science* **2008**, *319*, 1635–1638.
- (38) Kelly, T. F.; Larson, D. J. Atom probe tomography 2012. *Annu. Rev. Mater. Res.* **2012**, *42*, 1–31.